

PPPL- 5116

PPPL-5116

Progress toward Commissioning and Plasma Operation in NSTX-U

M. Ono, J. Chrzanowski, L. Dudek, S. Gerhardt, P. Heitzenroeder,
R. Kaita, J.E.Menard, E. Perry, T. Stevenson, R. Strykowski,
P. Titus, A. von Halle, M. Williams

February 2015



Princeton Plasma Physics Laboratory

Report Disclaimers

Full Legal Disclaimer

This report was prepared as an account of work sponsored by an agency of the United States Government. Neither the United States Government nor any agency thereof, nor any of their employees, nor any of their contractors, subcontractors or their employees, makes any warranty, express or implied, or assumes any legal liability or responsibility for the accuracy, completeness, or any third party's use or the results of such use of any information, apparatus, product, or process disclosed, or represents that its use would not infringe privately owned rights. Reference herein to any specific commercial product, process, or service by trade name, trademark, manufacturer, or otherwise, does not necessarily constitute or imply its endorsement, recommendation, or favoring by the United States Government or any agency thereof or its contractors or subcontractors. The views and opinions of authors expressed herein do not necessarily state or reflect those of the United States Government or any agency thereof.

Trademark Disclaimer

Reference herein to any specific commercial product, process, or service by trade name, trademark, manufacturer, or otherwise, does not necessarily constitute or imply its endorsement, recommendation, or favoring by the United States Government or any agency thereof or its contractors or subcontractors.

PPPL Report Availability

Princeton Plasma Physics Laboratory:

<http://www.pppl.gov/techreports.cfm>

Office of Scientific and Technical Information (OSTI):

<http://www.osti.gov/scitech/>

Related Links:

[U.S. Department of Energy](#)

[Office of Scientific and Technical Information](#)

Progress toward commissioning and plasma operation in NSTX-U *

M. Ono¹, J. Chrzanowski¹, L. Dudek¹, S. Gerhardt¹, P. Heitzenroeder¹, R. Kaita¹, J.E. Menard¹, E. Perry¹, T. Stevenson¹, R. Strykowski¹, P. Titus¹, A. von Halle¹, M. Williams¹, N.D. Atnafu¹, W. Blanchard¹, M. Cropper¹, A. Diallo¹, D.A. Gates¹, R. Ellis¹, K. Erickson¹, J. Hosea¹, R. Hatcher¹, S.Z. Jurczynski¹, S. Kaye¹, G. Labik¹, J. Lawson¹, B. LeBlanc¹, R. Maingi¹, C. Neumeyer¹, R. Raman², S. Raftopoulos¹, R. Ramakrishnan¹, L. Roquemore¹, S.A. Sabbagh³, P. Sichta¹, H. Schneider¹, M. Smith¹, B. Stratton¹, V. Soukhanovskii⁴, G. Taylor¹, K. Tresemer¹, A. Zolfaghari¹, and the NSTX-U Team.

¹ Princeton Plasma Physics Laboratory, PO Box 451, Princeton, NJ 08543, USA.

² University of Washington at Seattle, Seattle, WA 98195, USA.

³ Columbia University, New York, NY 10027, USA.

⁴ Lawrence Livermore National Laboratory, Livermore, CA 94551, USA.

E-mail contact of main author: mono@pppl.gov

Abstract. The National Spherical Torus Experiment - Upgrade (NSTX-U) is the most powerful spherical torus facility at PPPL, Princeton USA. The major mission of NSTX-U is to develop the physics basis for an ST-based Fusion Nuclear Science Facility (FNSF). The ST-based FNSF has the promise of achieving the high neutron fluence needed for reactor component testing with relatively modest tritium consumption. At the same time, the unique operating regimes of NSTX-U can contribute to several important issues in the physics of burning plasmas to optimize the performance of ITER. NSTX-U further aims to determine the attractiveness of the compact ST for addressing key research needs on the path toward a fusion demonstration power plant (DEMO). The upgrade will nearly double the toroidal magnetic field B_T of 1 Tesla (T) at a major radius of $R_0 = 0.93$ m, plasma current I_p of 2 mega-Amperes (MA) and NBI heating power of 14 MW. The anticipated plasma performance enhancement is a quadrupling of the plasma stored energy and near doubling of the plasma confinement time, which would result in 5 – 10 fold increase in the fusion performance parameter $n\tau T$. With $\beta_T \sim 25\%$ at $B_T = 1$ T, the absolute average plasma pressure in NSTX-U could become comparable to that of present-day tokamaks. A much more tangential 2nd NBI system, with 2-3 times higher current drive efficiency compared to the 1st NBI system, is installed to attain the 100% non-inductive operation needed for a compact FNSF design. With higher fields and heating powers, the NSTX-U plasma collisionality will be reduced by a factor of 3-6 to help explore the favorable trend in transport towards the low collisionality FNSF regime. NSTX-U first plasma is planned for March 2015, at which time the transition to plasma operations will occur.

1. Introduction

A significant upgrade of the National Spherical Torus Experiment facility [1,2] has entered its final construction phase, and preparation for plasma operations is now underway. The NSTX facility [3], which operated since 1999, has concluded its operation in 2011. The NSTX facility has been upgraded to enable significant enhancement in device and plasma parameters to address major NSTX-U missions. The major mission of NSTX-U is to develop the physics basis for an ST-based Fusion Nuclear Science Facility (FNSF) [4, 5]. The ST-based FNSF has the promise of achieving the high neutron fluence needed for reactor component testing with relatively modest tritium consumption. At the same time, the unique operating regimes of NSTX-U can contribute to several important issues in the physics of burning plasmas to optimize the performance of ITER. The NSTX-U program also aims to determine the attractiveness of the compact ST for addressing key research needs on the path toward a fusion demonstration power plant (DEMO).

2. Overview of NSTX-U Facility Capability

After over a decade of operations, the NSTX facility has undergone significant upgrades. Schematics of the NSTX and NSTX-U facilities are shown in Fig. 1, and their respective device and plasma parameters are shown in Table 1. The main changes are the replacement of the center-stack and the addition of the 2nd neutral beam injection (NBI) system. By removing the flex bus, the center-stack could be removed from NSTX. The new center-stack, shown in Fig. 2 with a much larger cross section inner TF coil, permits doubling of the TF from ~ 0.5 T to 1 T and the plasma current I_p from 1 MA and 2 MA while expanding the plasma pulse length from ~ 1 sec to 5 sec. As can be seen in the figure, NSTX-U retains the basic configuration of NSTX, as much of the NSTX facility is utilized including the vacuum vessel, and outer TF and PF coils. The outer TF legs and PF coils were originally designed to support the increased current levels. However, the vacuum vessel and associated magnetic field (outer TF and PF) coil support structures were enhanced in order to handle the anticipated 4x greater electromagnetic forces compared to NSTX. The addition of a 2nd NBI system (Fig. 3) will not only double the NBI heating power from 7 MW to 14 MW, but the strong tangential injection will increase the current drive efficiency by $\sim 1.5 - 2$ to enable non-inductive operation. The anticipated plasma performance enhancement is a quadrupling of the plasma stored energy and near doubling of the plasma confinement time, which would result in a 5 – 10 fold increase in the well-known fusion performance parameter $n\tau T$. Even though the device sizes remain relatively compact, with ~ 1 T toroidal magnetic fields and $\sim 25\%$ toroidal beta values, the absolute plasma pressure expected in the upgrade STs could be comparable to that of the present day tokamaks. This would assure that the exciting contributions of NSTX-U will continue to be at the forefront of the world fusion program.

3. Four Major Physics Goals of NSTX-U

The NSTX-U facility is designed to address four major physics goals/issues for tokamak/ST-based FNSF and fusion reactor systems [1,2]:

1. **Demonstration of stability and control for steady-state high β plasmas.** With the addition of the strongly tangential 2nd NBI beam system, NSTX-U is designed to attain 100% non-inductive operation at reactor-relevant high β plasmas. To achieve high bootstrap current fraction discharges, it is necessary to access to high β_N and high κ , i.e., $f_{BS} \propto A^{-0.5} (1+\kappa^2) \beta_N^2 / \beta_T$ where κ is the plasma elongation and β_N is a normalized beta. In Fig. 4, previously achieved κ and β_N values in NSTX are shown as triangles and squares, and operating points of various FNSF and pilot plant design studies are shown as diamonds [6]. The expected operating spaces of NSTX-U are shown as dotted squares. As can be seen from the figure, NSTX has achieved necessary $\kappa \sim 3$ and $\beta_N \sim 5$ needed for those facilities. The previous NSTX experiments have demonstrated $\sim 50\%$ bootstrap current fraction (f_{bt}) as required for FNSF and the non-inductive current fraction f_{NI} of up to 70%. With the expected electron energy confinement improvement due to the doubling of toroidal magnetic field, together with a factor of ~ 2 improved current drive efficiency of the second NBI system, 100% non-inductive operation should be attainable at ~ 1 MA plasma current in NSTX-U [2]. NSTX-U is also equipped with a set of six non-axisymmetric (3-D) control coils, which can be independently powered to actively control RWMs at high beta [7], control error fields [8], and apply resonant magnetic perturbations for plasma rotation [9] and ELM control [10].

2. Plasma energy confinement physics at low plasma collisionality, especially electron energy transport. In NSTX and MAST, the electron energy confinement has improved with reduced collisionality in H-mode plasmas [11,12]. Importantly, the lithium plasma facing component (PFC) coating also significantly improved electron energy confinement for H-mode plasmas in NSTX by $\sim 30\%$ [13]. This electron energy confinement improvement with lithium appears to be consistent with the favourable collisionality scaling [14]. Also in NSTX-U, the enhanced pedestal H-mode was observed to have an increase in the H-mode confinement factor H by $\sim 50\%$. With higher fields and heating powers, the NSTX-U plasma collisionality will be reduced by a factor of 3-6 to help explore the favorable trend in transport towards the low collisionality FNSF regime. The understanding of electron transport physics is especially critical for predominantly electron heated reactor plasmas, including ITER. If the favourable trends observed on NSTX hold at low collisionality, high fusion neutron fluences could be achieved in very compact ST devices as shown in Fig. 5 [1].

3. Divertor solutions for mitigating high heat flux. The total auxiliary heating power of 20 MW provided by the NBI and HHFW systems will allow NSTX-U to uniquely produce reactor-relevant high divertor heat fluxes of $\sim 40 \text{ MW/m}^2$. With the expected steady-state divertor heat flux limit for solid and liquid divertor PFCs to be $\leq 10 \text{ MW/m}^2$, it is essential to investigate innovative divertor heat mitigation concepts in NSTX-U. In NSTX, a snow-flake divertor configuration which provides divertor flux expansion of up to ~ 50 was investigated, demonstrating a significant divertor heat flux reduction of $\sim \times 3$ as shown in Fig. 6 [15]. In NSTX-U, the snow-flake configuration will be tested with an up-down symmetric configuration which should provide another factor of 2 heat flux reduction. NSTX-U will also continue to explore the use of lithium PFC coating techniques for enhanced plasma performance, and divertor power and particle handling [16, 17]. A lithium granular injector will be implemented for ELM pacing at high injection rate to control impurities and reduce the peak ELM heat flux.

4. Non-inductive start-up, ramp-up, and sustainment. With relatively small or no central OH solenoid capability expected in a compact lower aspect-ratio tokamak and/or ST reactors, it is crucial to demonstrate plasma start-up without use of a central solenoid. As shown in Fig. 7, the solenoid-free start-up, ramp-up, and sustainment scenario requires a number of tools including CHI, ECH, HHFW, and NBI as will be described in Sec. V. In NSTX, $\sim 160 \text{ kA}$ was successfully initiated with out an OH solenoid [18] and in NSTX-U, due to ~ 2.5 larger injector poloidal flux, $\sim 400 \text{ kA}$ of start-up current is anticipated [19]. With the $\sim 1 \text{ MW}$ level ECH heating, the CHI plasma is projected be heated to a few hundred eV. Target plasmas thus formed will be further heated with HHFW to a keV range and the NBI will be then applied for further current ramp-up and eventual sustainment of $\sim \text{MA}$ level plasma current at high beta, with $\sim 70\text{-}80\%$ bootstrap current fractions. The same scaling suggests $\sim 1\text{-}2 \text{ MA}$ of start-up current should be achievable in FNSF with CHI. At this current level, the main ($\sim 0.5 \text{ MeV}$) NBI heating and current drive can commence for current ramp-up and steady-state operation. It should be noted that another helicity injection concept termed Local Helicity Injection (LHI) is being developed on PEGASUS [20]. It successfully created a plasma current of $\sim 160 \text{ kA}$ in PEGASUS, and a gun for NSTX-U is under development to achieve $0.5 - 1.0 \text{ MA}$ of start-up plasma current. If successful, helicity injection can not only enable ST-based FNSF but also simplify the design of conventional aspect ratio tokamak reactors.

4. NSTX-U Upgrade Construction Project

4.1 New Center-Stack Fabrication

A schematic of the new center-stack is shown in Fig. 8. It is composed of an inner TF coil bundle, an OH solenoid, up-and-down symmetric PF 1a, 1b, and 1c coils, and a CS casing [21].

TF bundle fabrication - The inner TF bundle utilizes 36 wedge-shaped OFHC copper and the lead extension stubs from higher strength copper alloy (Cu–Cr–Zr). The fabrication of the TF bundle conductors was done by Major Tool in Indianapolis, Indiana. Each TF conductor requires a welded connection to a lead extension stub on both ends. Using a conventional copper weld or braze would soften (anneal) the metal and weaken the connection. A metal joining technique called friction stir welding which avoids annealing was employed at Edison Welding Institute in Columbus, Ohio. This joining technique preserves the copper material strength in the joint area. In Fig. 9, a completed TF conductor bar is shown. After arriving PPPL, a cooling passage with a copper tube was soldered into a length-wise groove on one side of the TF conductor wedge with a specially developed eutectic (96Sn/4Ag) solder paste formulated with non-ionic flux [22]. This utilization of non-ionic flux was motivated by the previous electrical insulation failure in the NSTX TF bundle, where the residual Zn-Cl based flux caused gradual deterioration of the insulation material over ~ 7 years of operations. Again, the soldering temperature was carefully controlled to avoid annealing the TF conductor. The assembly of the center-stack was carried out at a specially prepared coil shop with a clean preparation room and an oven room at PPPL. Each conductor was baked at 170°C to remove any excess flux. The conductor was then grit blasted and primed before the S-2 glass TF turn insulation was applied. A TF quadrant section was assembled with 9 conductors placed into a quadrant mold as shown in Fig. 10 (a). The quadrant construction was chosen to maintain the high tolerance required for the TF bundle. Each TF quadrant was successfully vacuum pressure impregnated (VPI) using the CTD resin system CTD 425, which is a 3 cyanate ester-epoxy blend with long service life and low viscosity to aid the impregnation process. The same CTD 425 was used throughout the VPI process for both the new center-stack TF and OH coils. The shear bond strength of the cured epoxy-glass composite is 40 MPa at 373°K . The four VPI'ed quadrants were then assembled together to complete the full TF bundle as shown in Fig. 10 (b). The full TF bundle is ground wrapped with S-2 glass tape before placed into a mold for VPI. The full TF bundle after VPI is shown in Fig. 10 (c)]. After completing the TF bundle in 2013, the winding of the OH coil over the full TF bundle was performed in 2014.

OH-Coil Winding - The upgraded OH coil is designed for 6077 V @ 24,000 A, providing poloidal flux of ~ 2.1 V-S which is ~ 3 x that of NSTX. The OH final conductor size is 15.5 mm x 16.8 mm extruded oxygen-free silver-bearing copper conductor with a 5.7 mm ID cooling passage. The 884 turn 4-layer OH coil was wound (2-in-hand) on a 2.5 mm thick cylinder of moldable mandrel material cast over the cured TF bundle. The OH coil design features a co-axial lead located near the center-stack pedestal support at the bottom end to minimize lead stresses due to thermal expansion. The OH conductor is first grit blasted and primed, similar to the TF conductors. Individual turns were insulated with co-wound glass/Kapton insulation applied in multiple half-lapped layers. The S-2 glass ground-wrap was applied over the finished wound coil. 32 in-line induction brazes were performed during the OH winding operations. Each braze joint was mechanically loaded (stretched) and helium leak tested to ensure a quality braze joint. In line brazes were also required at layer

to layer joints using a TIG-braze procedure similar to joints developed for the NSTX OH coil. The TIG-braze process consists of a torch braze utilizing a tungsten tipped arc welder with shielding gas. The OH coil wound in place on a 2.5 mm thick cylinder of moldable mandrel material cast over the cured TF bundle. The start of the OH coil winding is shown in Fig. 11(a). The Aquapour mandrel material is designed to easily wash away after coil curing to leave an air gap between the TF bundle and OH coil for thermal expansion and motion between the two coils. Once the Aquapour has been removed, the TF bundle is supported externally at the top and bottom of the Center Stack to center it within the OH coil. After the OH winding was completed, a VPI of the entire TF-OH center-bundle was successfully conducted as shown in Fig, 11 (b). It should be noted that after VPI, it was found that the epoxy penetrated the Aquapour. This epoxy saturation of the Aquapour made its removal by simply dissolving with water no longer possible. The impact of leaving the Aquapour in place on the NSTX-U operations was evaluated. The axial tension stress in the OH, generated due to the thermal growth of coils must be controlled by keeping the OH coil temperature at or above that of the TF. Based on the analyses of the NSTX-U plasma scenarios, it was concluded with a high degree of confidence that all of the NSTX-U physics objectives can be met with Aquapour in place. The presence of the Aquapour has some advantages of providing robust centering support for the OH with respect to the TF. The decision therefore was made to leave the material in place. The TF and OH coils were electrically tested successfully to full test voltages of 4.5 kV and 13 kV, respectively.

Final Center-Stack Assembly - In parallel, the Center-Stack Casing was fabricated by Martinez-Turek in California. After its arrival at PPPL, the 700 inconel studs were welded on its wall surface for mounting the carbon tiles to the walls. The graphite tiles (PFC) were mounted with surface diagnostics to the casing walls. There are inner poloidal field (PF) coils (PF1a, b, and c) and they were manufactured by Everson-Tesla in New Jersey. The completed OH/TF/PF1 bundle and CS casing were then transported to the NSTX-U Test Cell South Bay. After wrapping the TF/OH/PF1 bundle with Micro-therm thermal insulation, the CS casing was lowered onto the bundle to complete the CS assembly. The assembled CS was then lowered into the NSTX-U vacuum chamber in October 2014 as shown in Fig. 12. To complete the TF coil, the inner TF bundle will be connected to the outer TF legs using a high strength Cu-Zr copper alloy flex joint as shown in Figs 8 and 13. The flex joint has to accommodate the vertical cyclic movement due to the growth of the TF bundle (~ 1.7 cm) during the operation, while resisting the $j \times B$ force of ~ 130 kA of current through the joint. The TF flex connection was fabricated from a solid U-shaped copper alloy piece by making 16 precision parallel cuts via electric discharge machining by Zenez Precision of New Jersey. The flex joint has successfully passed a ~ 300,000 cycle fatigue test.

NSTX-U Device Structural Enhancements - In order to handle the anticipated 4x greater electromagnetic forces for NSTX-U, the vacuum vessel and associated magnetic field coil support structures must be enhanced accordingly. The umbrella structure reinforcements, and PF 2/3 support upgrade hardware and PF 4/5 support upgrade hardware enhancements were implemented. Two new outer TF legs were fabricated and installed to replace the ones with cooling water leak and electrical insulation issues. The outer TF leg support upgrades were also fabricated and installed. The TF-VV clevises to better support outer TF legs were welded onto the vessel. The new much more robust umbrella legs were installed on the machine. The vacuum vessel leg attachment connections were modified to clear the clevises. In addition, since the plasma disruption forces are also expected to increase by a factor of 4, the internal passive plates were reinforced by replacing the stainless steel attachment hardware with Inconel versions. The support structure enhancement activities are now complete.

Digital Coil Protection System - To protect NSTX-U from unintended operational conditions due to the power supplies delivering current combinations and consequential forces or stresses beyond the design-basis, a digital coil protection system (DCPS) is being implemented [23]. The DCPS is designed to prevent accidental (either human or equipment failure) overload beyond the design conditions of the structure which the power supply system could generate, even while each individual power supply is operating within its allowable current range as shown in Fig. 14. In the initial instance of DCPS, the algorithms will test approximately 125 force and stress calculations against limit values, using both two models for the plasma shape and two models for potential post-disruption currents; this results in 500 total force/stress calculations in addition to 14 thermal limit calculations. The update rate of each type will be 200 μ s for both the force-based and the thermal-based signals. Redundant current measurements for each coil and plasma current will be provided as inputs. This type of sophisticated coil protection system if fully demonstrated could be utilized for safe operation of future fusion devices including ITER.

Power system upgrades - The NSTX-U power systems include 68 identical rectifiers (Transrex AC/DC Convertors) providing a total pulsed power capability of 1650 MVA for 6 seconds every 300 seconds. New firing generators (FG) were installed for the precise control of thyristor firing angles needed for NSTX-U operations particularly critical for the 8-parallel, 130kA TF system configuration. The new FG delivers firing pulses with far greater resolution, precision, and repeatability than the previous ones in NSTX. In addition, a TF turn-to-turn fault detection and trip has been designed and installed. The NSTX-U 475 MVA / pulse motor generator with weld cracks was also repaired. The motor generator repair brought the motor generator to its original specifications, and the repair will enable the full operation of NSTX-U.

4.2 Neutral Beam Injection System Upgrade

The 2nd NBI upgrade scope is to add a complete, functional second beam-line (BL) to NSTX-U at aiming tangency radii of 110, 120, and 130 cm compared to 50, 60, and 70 cm for the present 1st NBI. A schematic of the present and new 2nd NBI systems are shown in Fig. 3. This task largely utilizes the existing TFTR NBI infrastructure. To accommodate the strongly tangential injection, a specially designed “bay-window” was installed as shown in Fig. 15 [24]. By moving the vacuum vessel wall out by \sim 12 cm, a potential issue of the clipping of the outer most beam by the vacuum vessel was avoided. The redesigned and relocated NBI armor to capture both sets of NBI heat deposition profiles while maintaining the same level of vacuum vessel wall protection is shown in Fig. 12 (b) [25]. The 2nd NBI tasks included the TFTR NBI BL tritium decontamination, refurbishments, sources, relocation, services, power and controls, and NSTX-U Test Cell (NTC) rearrangements. In addition, there are vacuum vessel (VV) modifications, the NBI and Torus Vacuum Pumping System ducts, and NBI armour shown in Fig. 12(b). The 2nd NBI BL (BL2) refurbishment and relocation have been completed. The BL box and lid were moved into the NTC and reassembled. The installation of the support structure and alignment of the BL has been completed. The refurbished 90 inch flange, ion dump, calorimeter, and bending magnet were installed on the BL. The source platform has been fully decontaminated and installed. Relocation also included moving three High Voltage Enclosures (HVEs) from the TFTR Test Cell Basement into the NTC. The High Voltage Transmission Lines were refurbished and

relocated to the NTC where they were installed on the HVE and Source connections. The three NB Ion Sources were installed on the BL2 platform and vacuum connections completed. The BL2 and its sources are ready for vacuum pump down. With the successful completion of the above tasks, preoperational testing of BL systems and BL2 power and controls has started to properly commission subsystems and confirm readiness for operations. This testing has begun in earnest in 2014 and flows into start up operations based on project schedules. An aerial view of the NSTX-U Test Cell in October 2014 is shown in Fig. 16 where the 2nd NBI system can be seen in the foreground. Pending appropriate approvals, the 2nd NBI upgrade project is scheduled to complete in January, 2015.

5. Additional Science Facility Enhancements

In addition to the above upgraded facility capability, there are other important research facility capability required to address the NSTX-U mission elements. Perhaps the most challenging and potentially most important one is the solenoid-free high beta operations required for the ST-based FNSF and power plants. This area of research also could benefit the advanced tokamak scenario development as well. The solenoid-free start-up is critical for the ST-based compact FNSF since there is no-room for the central solenoid and associated neutron shielding as described in Sec. 5.1. The current ramp-up to an intermediate current level with HHFW is highly important to bridge the gap between the start-up plasma and the minimum current level (~ 400 kA for NSTX-U and 1-2 MA for an ST-FNSF) required to turn on the main NBI beams for heating and current drive as described in Sec. 5.2. In Sec. 5.3, the resistive wall mode (RWM) stabilizing coils are described which are used to achieve high beta plasmas needed for high f_{BS} discharges without disruption. In Sec. 5.4, we describe the divertor heat flux mitigation tools. Finally, we will summarize the diagnostics being readied for NSTX-U in Sec. 5.5.

5.1 Solenoid-free Start-Up with CHI

For non-inductive start-up, the coaxial helicity injector (CHI) is prepared to support plasma start-up current of well over the 400 kA required to couple a CHI started discharge to non-inductive current ramp-up [19]. The baseline PFCs for the initial NSTX-U operation are graphite tiles. Because of the increased plasma heat loads due to the increased NBI heating power and pulse duration, it was decided to enhance the protection of the “CHI Gap”. The CHI Gap is the region between the NSTX-U inner and outer vacuum vessels, above or below the CHI insulators as shown in Figs. 12 (b) and 17 (a). The graphite tiles on both the inner and outer divertors will be extended downwards, coming in close contact to the PF-1C coil casing and stainless steel outer vessel flanges and shielding these components from plasma contact. This narrower and deeper CHI gap will protect the vessel and PF-1C coil from excessive heat flux and protect the plasma from metal contamination, while continuing to provide the capability for CHI operations. A comparison of the poloidal injector flux contours are shown for NSTX and NSTX-U in Fig. 17 (b). The injector flux is about 2.5 time larger for NSTX-U compared to that of NSTX. The enhanced injector flux should result in

proportionately larger start-up current. Due to the anticipated higher CHI start-up current and required bias-voltage (~ 3 kV in NSTX-U compared to ~ 2 kV in NSTX), the center-stack magnet insulation is enhanced accordingly. The electron cyclotron heating (ECH) at ~ 1 MW level will be implemented to heat the CHI created plasma to 200-300 eV range so that the HHFW electron heating and current ramp-up can couple into the CHI start-up plasma ~ 30 - 50 eV which maybe too cold for the HHFW Landau heating.

5.2 HHFW for Current Ramp-up

A 6 MW High-Harmonic Fast Waves (HHFW) system is being prepared for electron heating and current ramp-up [26]. While the HHFW system is basically unchanged, the antenna feed-thru conductors were modified to be able to handle the higher disruption loads ($\sim \times 4$) in NSTX-U. To handle those disruption loads, compliant connectors were designed, tested, and installed between the feed-throughs and antenna straps for the NSTX-U operation. In order to increase the power from the existing 12-strap HHFW antenna, the rf voltage stand-off was tested on an rf test stand with the new compliant feeds. The test demonstrated rf voltage stand-off of 46 kV, which is about twice the value required. The HHFW antenna system with the compliant feeds and improved back plate grounding were installed in NSTX-U, as shown in Figs. 12(b) and 18. The tests also showed rf-induced arc-prone areas behind the back-plate. For improved rf diagnostics, rf probes and tile sensors were also installed.

5.3 Tools for High-beta / High Bootstrap Current Fraction Operations

To support high beta NSTX-U operation, a number of macro-stability control tools are being prepared. Mid-plane RWM control coils (shown in Fig. 19), and equilibria require re-computation of $n = 1$ active RWM control performance using proportional gain, and RWM state space control [7]. The upgrade also adds new capability, such as independent control of the 6 RWM coils with 6 switching power amplifier (SPA) sources. This new capability, combined with the upgrade of the RWM state space controller will also allow simultaneous $n = 1$ and $n = 2$ active control, along with $n = 3$ dynamic error field correction. Finally, the active control performance of the proposed off-mid-plane non-axisymmetric control coils (NCC) also needs to be evaluated. A significant increase in controllable β_N is expected with the RWM state space control in NSTX-U, as was found for NSTX.

Disruption Mitigation Systems - A key issue for ITER, and the tokamak/ST line of fusion devices in general, is the avoidance and mitigation of disruptions. Most of the disruptions are expected to be mitigated by massive gas injection (MGI) [27]. In support of the planned MGI Experiments on NSTX-U, the University of Washington has successfully built and tested an electromagnetic MGI valve for installation on NSTX-U. The operating principle of the valve is similar to the valve that is being planned for ITER. The lower divertor valve and the mid-plane MGI valves will be installed on NSTX-U early in 2015. The valve is at present undergoing off-line tests at the Univ. of Washington. After these tests are completed later this year, three such valves will be built for installation on NSTX-U.

5.4 Novel Power Exhaust Solutions

In NSTX-U, the projected peak divertor heat fluxes can reach 20-40 MW/m² with $I_p \leq 2$ MA, $P_{\text{NBI}} \leq 12$ MW, with pulse length up to 5 sec. NSTX-U will explore novel solutions to boundary physics power exhaust challenge by testing so-called “snowflake” (SF) divertor configuration, and liquid metal plasma facing components to mitigate erosion and melting problems.

Snowflake Divertors - In NSTX-U, two (upper and lower) sets of four divertor coils will be used to test up-down-symmetric snowflake (SF) divertors as shown in Fig. 20 [28]. In NSTX, a single lower SF divertor was investigated as shown in Fig. 6 [9]. The modeling projections for the NSTX-U SF divertor geometry are favourable, showing large reductions in divertor T_e and T_i , as well as peak divertor heat fluxes due to the geometric and radiation effects, both with 4% of carbon impurity levels and with neon or argon seeding.

Lithium Application Tools - With encouraging results in NSTX [16, 29], a number of lithium application tools are being prepared for NSTX-U. Two downward-oriented lithium evaporators (LITERs) will be re-installed. An electron beam heated upper aiming evaporator to cover the upper divertor region is being developed. The electron beam enables Li to be promptly evaporated for rapidly providing fresh lithium coatings. A lithium granular injector (LGI) for ELM pacing which was successfully demonstrated on EAST, is being prepared for NSTX-U. The NSTX-U LGI system is capable of injecting horizontally-redirectioned spherical lithium granules (0.6 mm) at speeds approaching 100 m/s. It is anticipated that much higher pacing frequencies can eventually be achieved using the basic injector technology. Granule feeding rates (pacing frequencies) of 500 Hz have been achieved in the laboratory tests.

5.5 Diagnostic systems

The NSTX-U diagnostic installation has been an active area of NSTX-U operational preparation. A list of the diagnostic systems which are expected to be available for NSTX-U within the first year of operation is shown in the Table 2 except for the poloidal FIR high-k scattering system, which is expected in FY 2016. Most of the NSTX diagnostics were re-installed (in black), some are significantly enhanced (in blue) and new ones were added (in red). We note that at least half of those diagnostic systems have strong collaboration components. The in-vessel diagnostic installation and related calibration tasks have been complete.

6. NSTX-U Plasma Operation Start-Up Planning

An operational plan toward full NSTX-U operational capability is being developed. A draft plan is shown in Table 2, based on assessment of physics needs for the first year of operations. The 1st year goal is to operate NSTX-U with the electromagnetic forces ($I_p B_T$) at halfway between NSTX and NSTX-U limits and 50% of the NSTX-U design-point of heating of the TF coil. This still allows NSTX to operate at $B_T \sim 0.8$ T, $I_p \sim 1.6$ MA, and a maximum flat-top duration of 3.5 s in the first year, which is far beyond the achieved NSTX parameters. The device will be inspected and refurbished as needed at the end of the each operating year. For the second year, the toroidal magnetic field will be increased to its full field value of 1 T but with the heating of the TF coil kept to 75% of the design-point. This will allow 3 sec discharges at full field and current. The same limits should allow the full 5 sec discharges at $B_T \sim 0.8$ T and $I_p \sim 1.6$ MA. The device will be brought to full operational capability in the third year of NSTX-U operation.

7. Discussions and Conclusions

The NSTX upgrade construction project has entered its last phase, and preparation for plasma operations is now underway. The major mission of NSTX-U is to develop the physics basis for a compact ST-based Fusion Nuclear Science Facility (FNSF). At the same time, the unique operating regimes of NSTX-U can contribute to several important issues in the physics of burning plasmas to optimize the performance of ITER. The NSTX-U program further aims to determine the attractiveness of the compact ST for addressing key research needs on the path toward a fusion demonstration power plant (DEMO). The new center-stack will provide $B_T = 1$ Tesla (T) at a major radius of $R_0 = 0.93$ m compared to 0.55 T at $R_0 = 0.85$ m in NSTX, and will enable a plasma current I_p of up to 2 mega-Amperes (MA) for 5 sec compared to the 1 MA for 1 sec in NSTX. A much more tangential 2nd NBI system, with 2-3 times higher current drive efficiency compared to the 1st NBI system, has been installed. NSTX-U is designed to attain the 100% non-inductive operation needed for a compact FNSF design. NSTX-U first plasma is planned for the spring of 2015, at which time the transition to plasma operations will occur.

***Acknowledgments:** This work was supported by DoE Contract No. DE-AC02-09CH11466.

References:

- [1] MENARD, J.E., et al., *Nucl. Fusion* **52**, 083015 (2012).
- [2] GERHARDT, S.P., et al., *Nucl. Fusion* **52**, 083020 (2012).
- [3] ONO, M., et al., *Nuclear Fusion* **40**, 557 (2000).
- [4] PENG, Y-K.M., et al., *Fusion Sci. Technol.* **60**, 441 (2011).
- [5] MENARD, J.E., et al., 2014 *IAEA Fusion Energy Conference* FNS/1-1.
- [6] GERHARDTY, S.P., et al., *Nucl. Fusion* **51** 073031 (2011).
- [7] S. A. SABBAGH, S.A., et al., *Nucl. Fusion* **53**, 104007 (2013)
- [8] PARK, J-K., et al., *Nucl. Fusion* **52**, 023004 (2012).
- [9] ZHU W., et al., *Phys. Rev. Letters* **96**, 225002 (2006).
- [10] CANIK, J.M. et al., *Phys. Rev. Lett.* **104**, 045001 (2010).
- [11] KAYE, S.M., et al., *Nucl. Fusion* **47** 499 (2007).
- [12] VALVONIC M., et al., *Nucl. Fusion* **51** 073045 (2011).
- [13] MAINGI, R., et al., *Nucl. Fusion* **52** 083001 (2012).

- [14] KAYE, S.M., et al., *Nucl. Fusion* **53** 063005 (2013)
- [15] SOUKHANOVSII, V.A., et al., *Phys. Plasmas* **19**, 082504 (2012).
- [16] GRAY, T.K., et al., *Nucl. Fusion* **54**, 023001 (2014).
- [17] ONO, M., et al., *Nucl. Fusion* **53**, 113030 (2013).
- [18] RAMAN, R., et al., *Phys. Rev. Lett.* **97**, 175002 (2006).
- [19] RAMAN, R., et al., *IEEE Transactions on plasma science* **42**, 2154 (2014).
- [20] BATTAGLIA, D.J. et al., *Phys. Rev. Lett.* **102**, 225003 (2009).
- [21] DUDEK, L., et al., *Fusion Engineering and Design* **87**, 1515 (2012).
- [22] JURCZYNSKI, S. Z., et. al. 2013 *IEEE 25th Symposium on Fusion Engineering (SOFE)*.
- [23] ERICKSON, K.G., et al., *IEEE Transactions on plasma science* **42**, 1811 (2014).
- [24] ATNAFU, N.d., et al., 2013 *IEEE 25th Symposium on Fusion Engineering (SOFE)*.
- [25] TRESEMER, K. et al., *Fusion Science and Technology* **60**, 303 (2011).
- [26] ELLIS, R., et al., *AIP Conference Proceedings, 20th Topical Conference on Radiofrequency Power in Plasmas*, **1580**, 350 (2014).
- [27] RAMAN, R., et al., *Review of Scientific Instruments*, **85** 11E801 (2014).
- [28] SOUKHANOVSII, V.A., et al., 2012 *IAEA Fusion Energy Conference EX/P5-21*.
- [29] ONO, M., et al., *Fusion Engineering and Design* **87**, 1770 (2012).

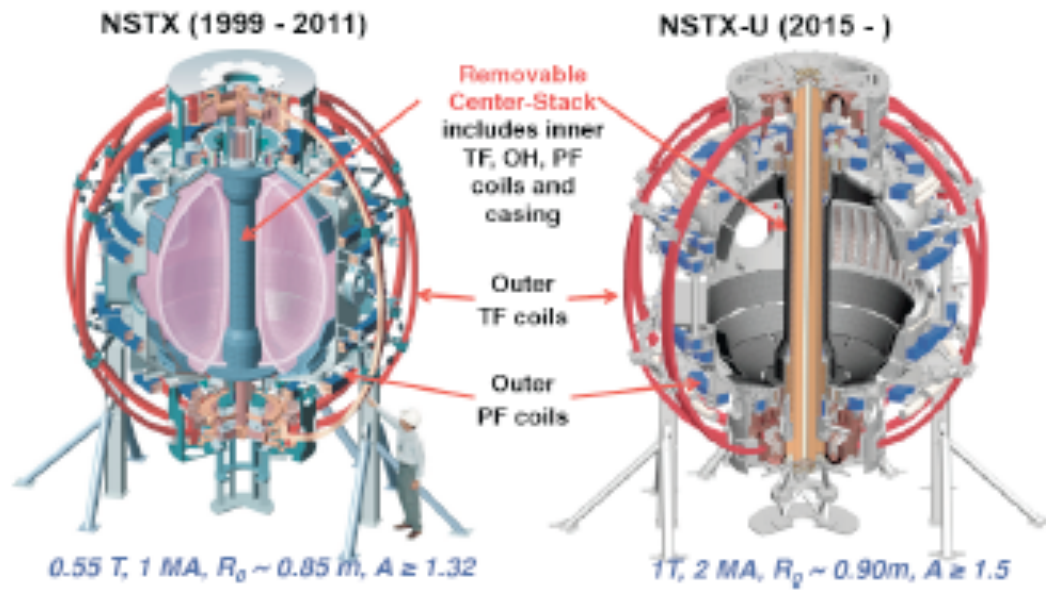


FIG. 1. Schematics of NSTX and NSTX-U devices.

TABLE 1: NSTX and NSTX U Parameters

	R_0 (m)	A_{ext}	I_p (MA)	B_T (T)	t_{IT} (s)	R_{CS} (m)	R_{OH} (m)	OH flux (Wb)
NSTX	0.854	1.32	1	0.55	1	0.185	1.574	0.75
NSTX-U	0.934	1.5	2	1	6.5	0.315	1.574	2.1

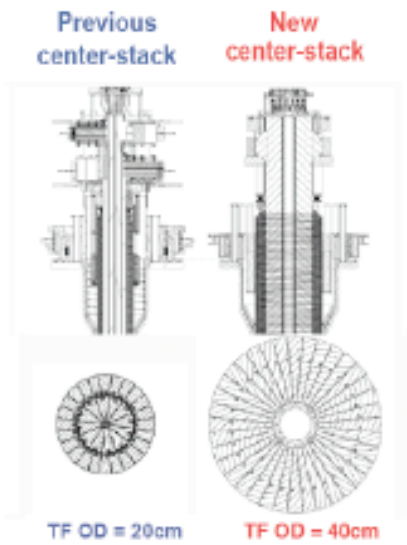


FIG. 2. Schematics of NSTX and NSTX-U center-stack with inner TF coil cross section views..

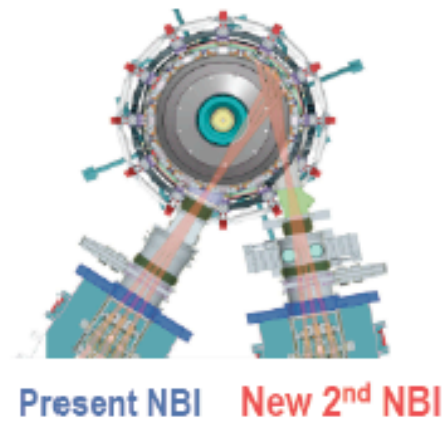


FIG. 3. Schematics of present and 2nd NBI systems on NSTX-U.

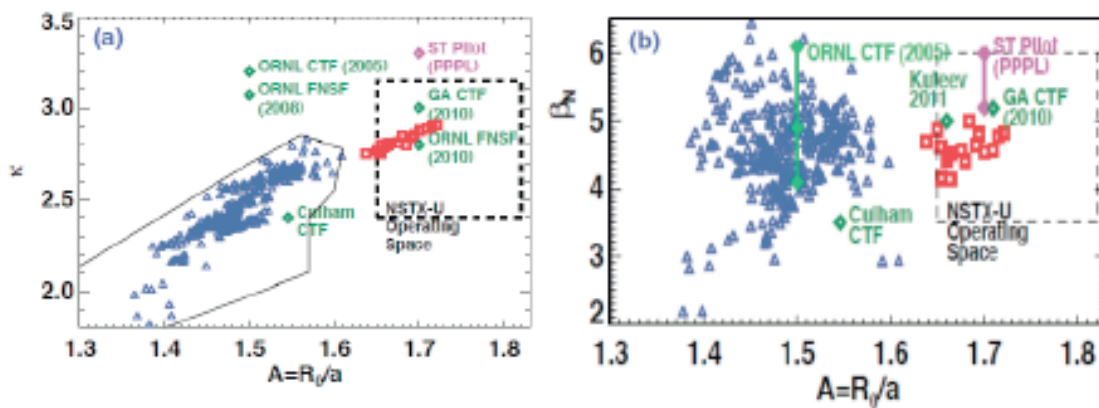


FIG. 4. Bootstrap current relevant parameters $\kappa - 3$ and β_N achieved in NSTX. The FNSF and polot plant operating parameters are as labels. The expected NSTX-U operational spaces are indicated by the dotted squares. .

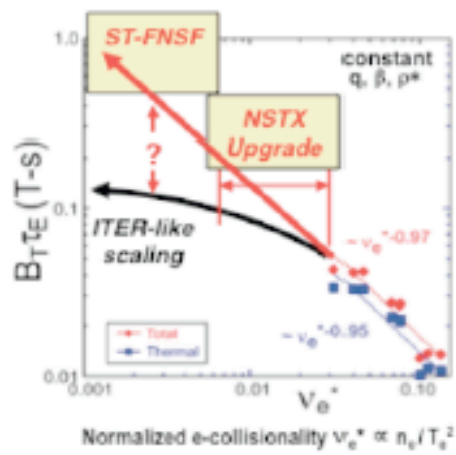


FIG. 5. Energy confinement time vs electron collisionality in NSTX.

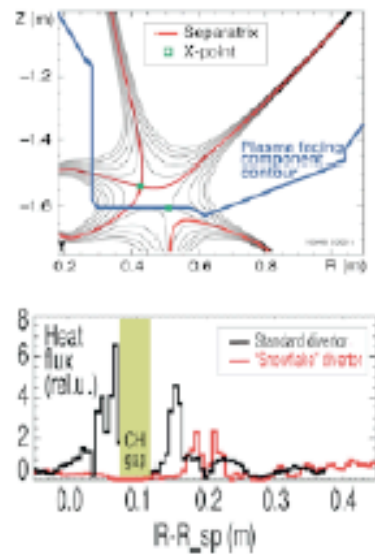


FIG. 6. Snow-flake divertor configuration (above) and measured divertor flux comparison with standard configuration..

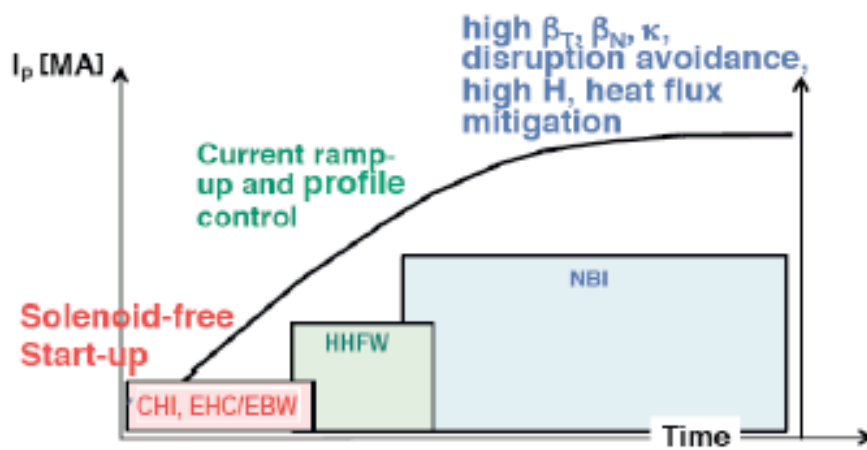


FIG. 7. A schematic for the fully non-inductive operation scenario in NSTX-U.

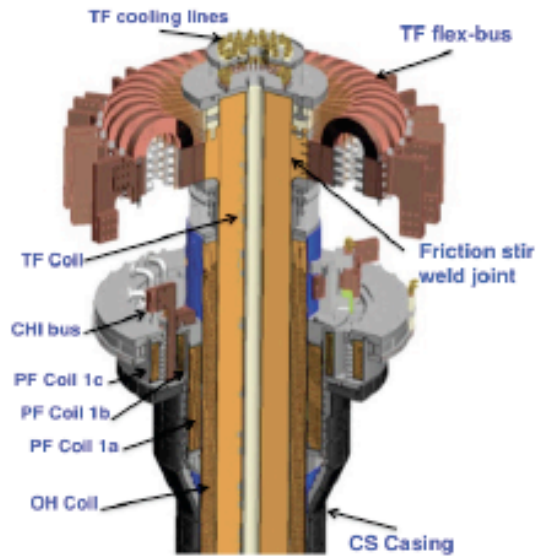


FIG. 8. A schematic of the new center-stack and the TF joint area..

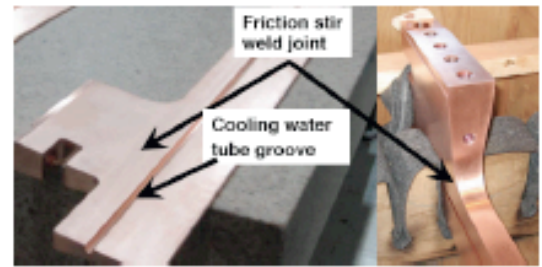


FIG. 9. A TF bar with friction stir welded lead extension and cooling tube groove.

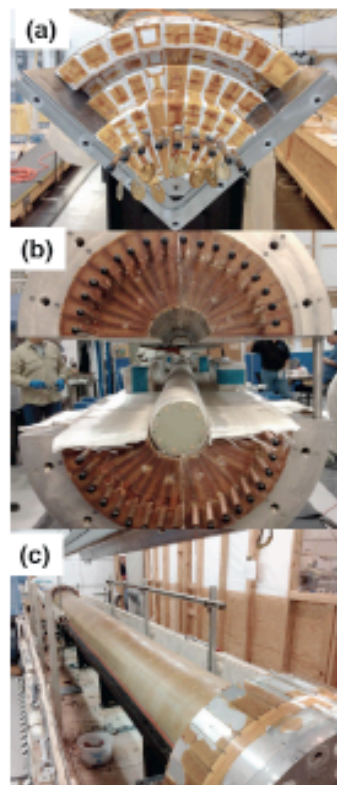


FIG. 10. TF fabrication stages (a) insulated TF quadrant prior to VPI (b) assembly of full bundle, (c) TF bundle after VPI.

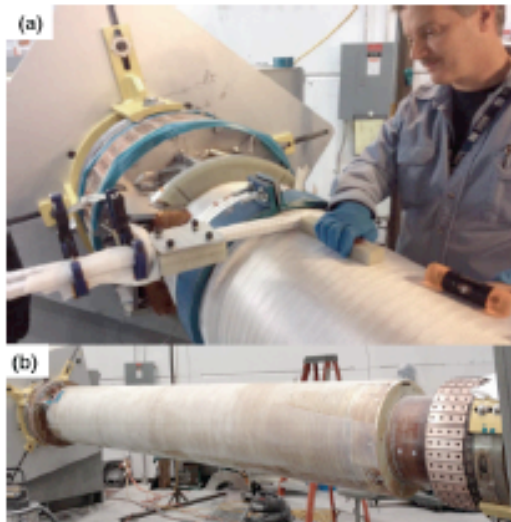


FIG. 11. OH Winding (a) Start of the two-in-hand OH winding. (b) Completed OH coil after VPI.

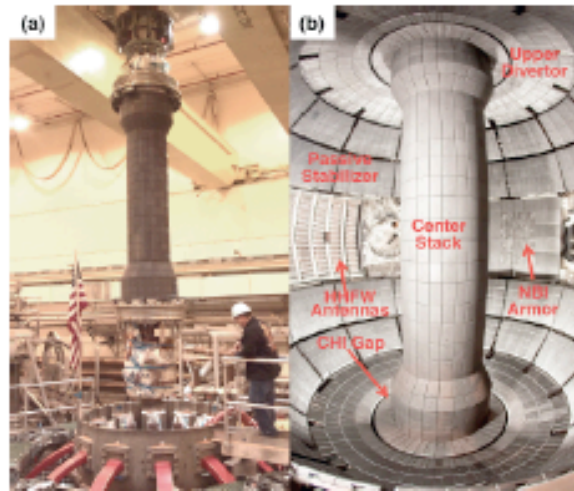


FIG. 12. (a) NSTX-U center-stack lowering to the vacuum vessel. (b) NSTX-U Center-stack installed.

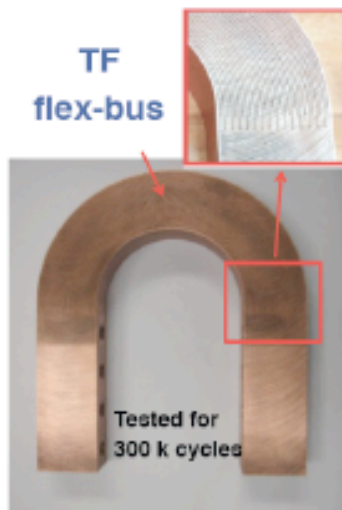


FIG. 13. NSTX-U TF flex bus with EDM cuts

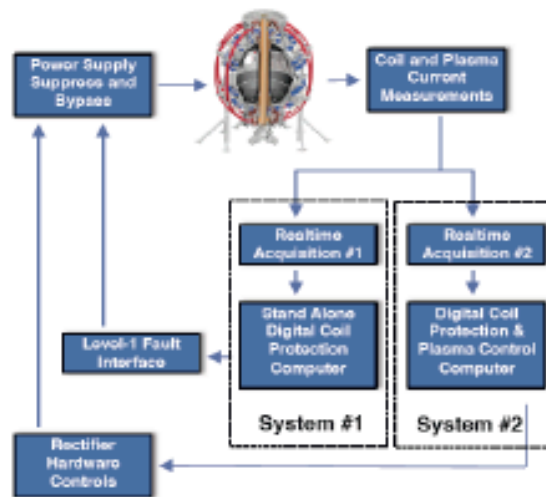


FIG. 14. Schematic of the NSTX-U Digital Coil Protection System providing comprehensive coil protection against electromagnetic loads and thermal limits.



FIG 15. *In-vessel view of the tangential injection port of the 2ndNBI.*

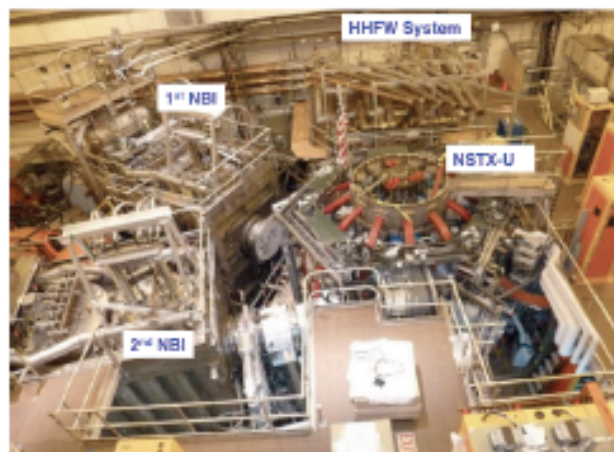


FIG 16. *In-vessel view of the tangential injection port of the 2ndNBI.*

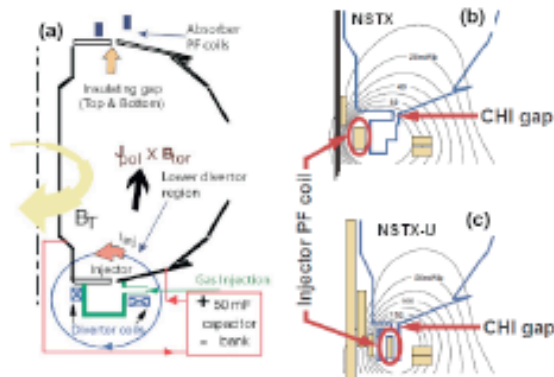


FIG. 17. NSTX-U CHI schematics. (a) A schematic of CHI set-up where the center-stack is electrically biased against outer vacuum vessel. The electrical discharge established is expelled into the main chamber by the $j_{pol} \times B_T$ force. (b) and (c) A comparison of poloidal flux pattern between NSTX and NSTX-U.

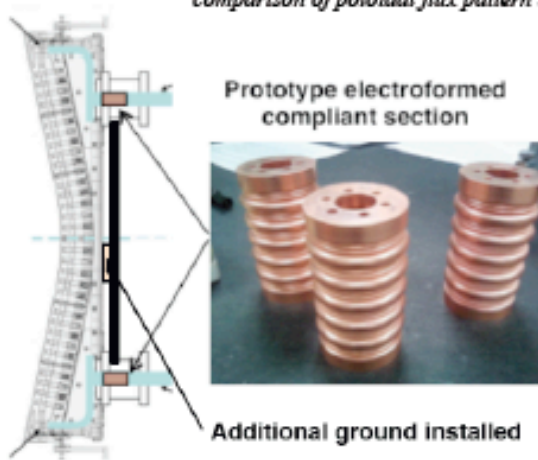


FIG. 18. A schematic of HHFW antenna with improved antenna feeds and backplate ground.

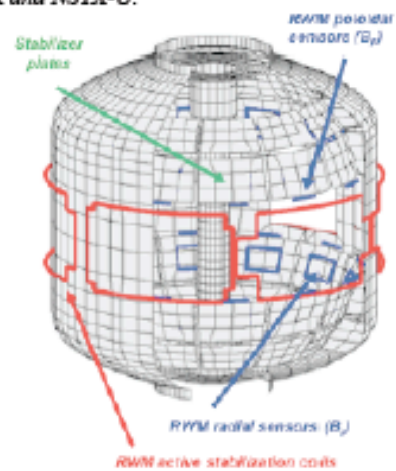


FIG. 19. Diagram of NSTX showing internal B_r and B_p sensors, passive stabilizing plates and ex-vessel 3-D control coils.

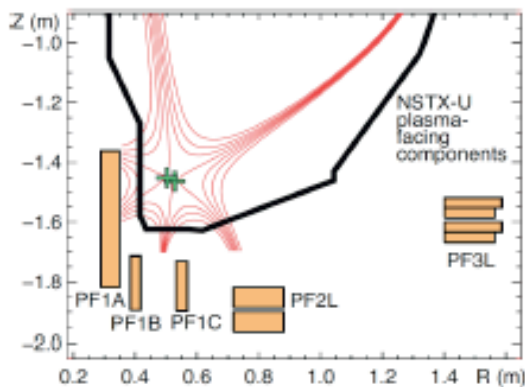


FIG. 20. Snow-flake Divertor configuration in NSTX-U.

TABLE 2: NSTX-U Diagnostics

<p>MHD/Magnetics/Reconstruction Magnetics for equilibrium reconstruction <i>Halo current detectors</i> <i>High-n and high-frequency Mirnov arrays</i> Locked-mode detectors RWM sensors</p> <p>Profile Diagnostics MPTS (42 ch, 60 Hz) T-CHERS: $T_e(r)$, $V_e(r)$, $n_C(r)$, $n_U(r)$, (51 ch) P-CHERS: $V_e(r)$ (71 ch) MSE-CIF (18 ch) MSE-LIF (20 ch) ME-SXR (40 ch) Midplane tangential bolometer array (16 ch)</p> <p>Turbulence/Modes Diagnostics <i>Poloidal FIR high-k scattering</i> <i>Beam Emission Spectroscopy (48 ch)</i> Microwave Reflectometer, <i>Microwave Polarimeter</i> Ultra-soft x-ray arrays – multi-color</p> <p>Energetic Particle Diagnostics <i>Fast Ion D_α profile measurement (perp + tang)</i> Solid-State neutral particle analyzer Fast lost-ion probe (energy/pitch angle resolving) Neutron measurements <i>New capability, Enhanced capability</i></p>	<p>Edge Divertor Physics Gas-puff Imaging (500kHz) Langmuir probe array Edge Rotation Diagnostics (T_e, V_e, V_{pol}) 1-D CCD H_α cameras (divertor, midplane) 2-D divertor fast visible camera Metal foil divertor bolometer AXUV-based Divertor Bolometer IR cameras (30Hz) (3) Fast IR camera (two color) Tile temperature thermocouple array Divertor fast eroding thermocouple Dust detector Edge Deposition Monitors Scrape-off layer reflectometer Edge neutral pressure gauges Material Analysis and Particle Probe Divertor VUV Spectrometer</p> <p>Plasma Monitoring FIReTIP interferometer Fast visible cameras Visible bremsstrahlung radiometer Visible and UV survey spectrometers VUV transmission grating spectrometer Visible filterscopes (hydrogen & impurity lines) Wall coupon analysis</p>
--	---

TABLE 3: NSTX-U Device Ramp-up Plan.

	NSTX (Max.)	FY 2015 NSTX-U Operations	FY 2016 NSTX-U Operations	FY 2017 NSTX-U Operations	Ultimate Goal
I_p [MA]	1.2	~1.6	2.0	2.0	2.0
B_T [T]	0.55	~0.8	1.0	1.0	1.0
Allowed TF I^2t [MA ² s]	7.3	80	120	160	160

Princeton Plasma Physics Laboratory Office of Reports and Publications

Managed by
Princeton University

under contract with the
U.S. Department of Energy
(DE-AC02-09CH11466)

P.O. Box 451, Princeton, NJ 08543
Phone: 609-243-2245
Fax: 609-243-2751

E-mail: publications@pppl.gov

Website: <http://www.pppl.gov>